

Hydrogen evolution reaction between small-sized Zr_n (n=2-5) clusters and water based on density functional theory

Lei-Lei Tang(唐雷雷), Shun-Ping Shi(史顺平), Yong Song(宋永), Jia-Bao Hu(胡家宝), Kai Diao(刁凯), Jing Jiang(蒋静), Zhan-Jiang Duan(段湛江), and De-Liang Chen(陈德良)

Citation: Chin. Phys. B, 2023, 32 (**6**): 066106. DOI: 10.1088/1674-1056/aca7ec

Journal homepage: http://cpb.iphy.ac.cn; http://iopscience.iop.org/cpb

What follows is a list of articles you may be interested in

Probing the effects of lithium doping on structures, properties, and stabilities of magnesium cluster anions

Xiao-Yi Zhang(张小义), Ya-Ru Zhao(赵亚儒), Hong-Xing Li(李红星), Kai-Ge Cheng(成凯格), Zi-Rui Liu(刘子锐), Zhi-Ping Liu(刘芷萍), and Hang He(何航)

Chin. Phys. B, 2023, 32 (**6**): 066102. DOI: 10.1088/1674-1056/acc51f

Structural and thermodynamic properties of inhomogeneous fluids in rectangular corrugated nano-pores

Yanshuang Kang(康艳霜), Haijun Wang(王海军), and Zongli Sun(孙宗利)

Chin. Phys. B, 2022, 31 (**5**): 056104. DOI: 10.1088/1674-1056/ac4237

Probing structural and electronic properties of divalent metal Mg_{n+1} and $SrMg_n$ (n = 2–12) clusters and their anions

Song-Guo Xi(奚松国), Qing-Yang Li(李青阳), Yan-Fei Hu(胡燕飞), Yu-Quan Yuan(袁玉全), Ya-Ru Zhao(赵亚儒), Jun-Jie Yuan(袁俊杰), Meng-Chun Li(李孟春), and Yu-Jie Yang(杨雨杰)

Chin. Phys. B, 2022, 31 (**1**): 016106. DOI: 10.1088/1674-1056/ac04aa

First-principles study of structural and opto-electronic characteristics of ultra-thin amorphous carbon films

Xiao-Yan Liu(刘晓艳), Lei Wang(王磊), and Yi Tong(童祎)

Chin. Phys. B, 2022, 31 (**1**): 016102. DOI: 10.1088/1674-1056/ac0cd8

A novel two-dimensional SiO sheet with high-stability, strain tunable electronic structure, and excellent mechanical properties

Shijie Liu(刘世杰) and Hui Du(杜慧)

Chin. Phys. B, 2021, 30 (**7**): 076104. DOI: 10.1088/1674-1056/abf34d

---

Hydrogen evolution reaction between small-sized Zr_n ($n = 2$–5) clusters and water based on density functional theory

Lei-Lei Tang(唐雷雷)[1], Shun-Ping Shi(史顺平)[1,†], Yong Song(宋永)[1,‡], Jia-Bao Hu(胡家宝)[1], Kai Diao(刁凯)[1], Jing Jiang(蒋静)[1], Zhan-Jiang Duan(段湛江)[1], and De-Liang Chen(陈德良)[2]

[1] *College of Mathematics and Physics, Chengdu University of Technology, Chengdu* 610059, *China*
[2] *School of Physics and Electronics, Guizhou Education University, Guiyang* 550018, *China*

(Received 26 September 2022; revised manuscript received 14 November 2022; accepted manuscript online 2 December 2022)

Density functional theory (DFT) is used to calculate the most stable structures of Zr_n ($n = 2$–5) clusters as well as the adsorption energy values of Zr_n ($n = 2$–5) clusters after adsorbing single water molecule. The results reveal that there is a significant linear relationship between the adsorption energy values and the energy gaps of the Zr_n ($n = 2$–5) clusters. Furthermore, the calculations of the reaction paths between Zr_n ($n = 2$–5) and single water molecule show that water molecule can react with Zr_n ($n = 2$–5) clusters to dissociate, producing hydrogen, and O atoms mix with the clusters to generate Zr_nO ($n = 2$–5), all of which are exothermic reactions. According to the released energy, the Zr_4 cluster is the most efficient in Zr_n ($n = 2$–5) clusters reacting with single water molecule. The natural population analysis (NPA) and density of states (DOS) demonstrate the production of hydrogen and orbital properties in different energy ranges, respectively, jointly forecasting that Zr_nO ($n = 2$–5) will probably continue to react with more water molecules. Our findings contribute to better understanding of Zr's chemical reactivity, which can conduce to the development of effective Zr-based catalysts and hydrogen-production methods.

Keywords: density functional theory, hydrogen evolution reaction, NBO analysis, reaction pathways

PACS: 61.46.Bc **DOI:** 10.1088/1674-1056/aca7ec

1. Introduction

Clusters are microscopic or submicroscopic aggregates formed by the physical or chemical bonding of several or even thousands of atoms, molecules, or ions. The physical and chemical characteristics of clusters vary with the number of atoms present, differing from those of single atom or molecule, and cannot be obtained by their epitaxy. Owing to their potential utility as functional nanomaterials, electronic components, and nanocatalysts, transition metal atomic clusters have been substantially studied experimentally and theoretically in recent years.[1,2] A surge in studies into hydrogen preparation has emerged recently because of the critical need for sustainable energy in the global community.[3–6] Therein, the hydrogen evolution reaction (HER) between metal clusters and water has been a research hotspot as a potential hydrogen energy preparation method. For example, Zhou *et al.*[7] investigated the reaction mechanism between small Ce clusters and single water molecule, and they discovered that the three clusters were all capable of easily dissociating water molecules. The interactions of Ge_7 and Ge_6Al clusters with water to create hydrogen were explored by Lei *et al.*[8] According to the first-principles, Li *et al.* calculated the chemical reaction pathways of Al_6Si and Al_6Cu clusters for hydrogen extraction from water molecules.[9,10]

The zirconium atom is a typical of 4d transition metal with an electronic configuration of $4d^25s^2$.[11] Metal zirconium and its compounds are frequently utilized as nuclear reactor structural materials,[12–16] refractory materials,[17–20] and catalyst materials[21–24] because of their excellent properties. Meanwhile, zirconium and zirconium-based clusters have been widely studied as an excellent hydrogen storage material.[11,25–27] Sheng *et al.* investigated the evolutions of small Zr clusters and the dissociative chemisorption of H_2 on Zr clusters.[11] The structures and electronic properties of $(ZrH_2)_n$ ($n = 5$–24) clusters were analyzed and evaluated based on density functional theory by Huang *et al.*[25] According to the density functional theory and coupled cluster methods, Syzgantseva *et al.* theoretically explored the dissociation of H_2 on ZrO_2 molecular clusters, which reacted to generate ZrO and water.[26] Although Zr clusters are widely used in the field of hydrogen storage, Zr clusters have not been utilized to extract hydrogen from H_2O so far.

In this work, we verify that Zr_n ($n = 2$–5) clusters can react with water, dissociate and produce hydrogen by hypothesis and calculation. We repeat the previous studies on Zr_n ($n = 2$–5) clusters structures[11,28,29] and select the stable structure with the lowest energy from various configurations. We will pay special attention to the HER mechanism of reaction between a single water molecule and Zr_n ($n = 2$–5) clusters. Through calculated reaction paths, we can directly see how the

†Corresponding author. E-mail: shishunping13@cdut.edu.cn
‡Corresponding author. E-mail: syong@cdut.edu.cn

© 2023 Chinese Physical Society and IOP Publishing Ltd

Zr_n ($n = 2$–5) clusters extract H_2 from water molecules. Our finding provides a more in-depth understanding of the chemical reaction properties of Zr, which may pave the way for developing more effective Zr-based catalysts.

2. Computational method

All the calculations were performed with B3LYP functional based on density functional theory (DFT), which is a combination functional of Becke's three parameter exchange functional (B3)[30,31] with the Lee–Yang–Parr (LYP)[32] generalized gradient correction functional. The LANL2DZ[29,33–37] basis set was used for Zr atoms, while the 6-311++G (3df, 3pd)[38] basis set was used for O and H atoms. To begin with, we performed optimization and frequency analysis of various isomers of Zr_n ($n = 2$–5) clusters to determine the most stable structures. Then, under the premise of fully considering different adsorption structures, single water molecule was adsorbed to different adsorption sites of the ground state structures of Zr_n ($n = 2$–5) clusters respectively and the structure optimization and frequency analysis were carried out. The most stable structure after adsorption (represented by $Zr_n@H_2O$) was obtained and selected for subsequent research. Following that, the initial guessed structure of the transition state was optimized and frequency was analyzed by Bernie's algorithm to calculate the transition state structure. The structures of reactants and products were determined by forward and reverse intrinsic reaction coordinates (IRC). Finally, the natural population analysis (NPA) charges of the products were calculated to study their electronic properties. All calculation results are achieved with Gaussian 16 program.[39]

3. Results and discussion

3.1. Stable structure of Zr_n (n = 2–5) clusters and $Zr_n@H_2O$ (n = 2–5) clusters

Since the electronic configuration of Zr_n ($n = 2$–5) cluster is a closed shell, we consider four spin multiplicities (1, 3, 5, 7) and different geometries to calculate the most stable structure of Zr_n ($n = 2$–5) cluster. Previous studies of the most stable structure of Zr clusters are repeated,[11,28,29] and the results are in good agreement with each other. As shown in the Fig. 1, there is no doubt that the most stable structure of Zr_2 cluster is linear, and the most stable structure of the Zr_3 cluster is triangular. The stable structures of clusters tend to be three-dimensional when the number of atoms in the cluster reaches four or more. The Zr_4 cluster's most stable structure is tetrahedron-like, while the Zr_5 cluster's most stable structure is triangular bipyramid.

On the basis of the stable structures, the symmetry is fully considered, and single water molecules are adsorbed to different adsorption sites, and then the structure optimization and frequency analysis are carried out to obtain the stable structure after adsorption as shown in Fig. 2. The ability of clusters to collect water molecules is measured by adsorption energy. The following formula is used to compute the adsorption energy:

$$E_a = E_{Zr_n@H_2O} - E_{Zr_n} - E_{H_2O}, \tag{1}$$

and the results are listed in Table 1.

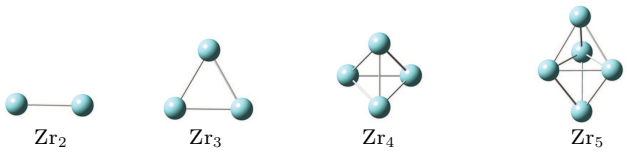


Fig. 1. Stable structures of Zr_n ($n = 2$–5) clusters.

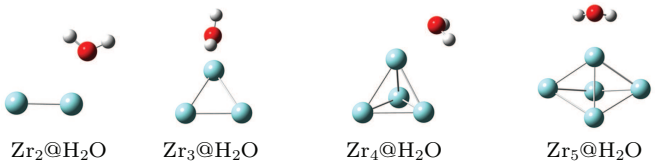


Fig. 2. Stable structures after adsorption of single water molecule.

Table 1. Adsorption energy values of $Zr_n@H_2O$.

Reaction	E_{Zr_n} (eV)	$E_{Zr_n@H_2O}$ (eV)	Adsorption energy (eV)
Zr_2	–4609.581	–4610.341	–0.760
Zr_3	–5875.761	–5876.517	–0.756
Zr_4	–7143.137	–7143.667	–0.530
Zr_5	–8410.157	–8410.820	–0.663

Based on the data of adsorption energy in Table 1, combining previous studies[25] on the energy gap of Zr clusters, we speculate that there is a certain correlation between the adsorption energy and the energy gap of the cluster. We use the following formula to calculate the correlation coefficient between the adsorption energy and the energy gap and obtain a result of -0.9558, which indicates that there is a strong negative linear correlation between the energy gap[28] of the cluster and the adsorption energy:

$$r = \frac{\sum_{i=1}^{n}(X_i - \bar{X})(Y_i - \bar{Y})}{\sqrt{\sum_{i=1}^{n}(X_i - \bar{Y})^2}\sqrt{\sum_{i=1}^{n}(X_i - \bar{Y})^2}}. \tag{2}$$

3.2. Reaction paths between H_2O and Zr_n (n = 2–5) clusters

We evaluate the overlap of natural bond orbital (NBO)[40] donor and acceptor (NBO by Multiwfn[41] and VMD[42]) of $Zr_n@H_2O$, which is generated by adsorption of single water molecule on Zr_n cluster, in order to clarify whether the electronic transfer appears between water molecules and Zr_n ($n =$ 2–5 clusters). For $Zr_2@H_2O$ as shown in Fig. 3, the strongest

interaction between Zr_2@H_2O results from the charge transfer of LPO_3 →LP*Zr_1, which is much stronger than that of BDO_3-H_4/BDO_3-H_5 →LP*Zr_1. Furthermore, we calculate the reaction paths between Zr_2 cluster and single water molecule, and the final products are Zr_2O+H_2. As shown in Fig. 4, the complete reaction process can be divided into the three steps that are described as follows. In the first step of reaction, an OH bond of the water molecule is broken in the process from A to TS1, and the H atom gradually approaches the middle of the two Zr atoms, forming an intermediate product B. It can be seen that the first H atom of water molecule is easy to dissociate. In the second step of reaction, the position of the H atom dissociated in the first step keeps moving, and the OH radical gradually moves to the middle of the two Zr atoms, forming an intermediate product C. The O atoms tend to be fixed and adsorbed between two Zr atoms. In the third step of the reaction, when the two H atoms are close to one another, the transition product TS3 is generated. In the process from TS3 to D, the two H atoms approach each other, forming H_2 finally. The whole reaction releases 2.59 eV of energy. On the whole, single water molecule and Zr_2 cluster are relatively easy to react and dissociate to generate hydrogen.

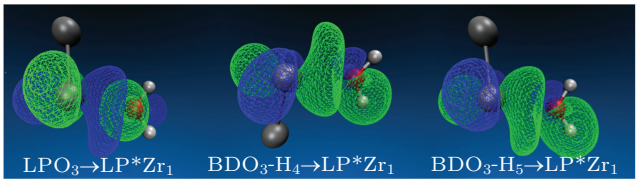


Fig. 3. Main NBO donor–acceptor overlaps between Zr_2 and H_2O.

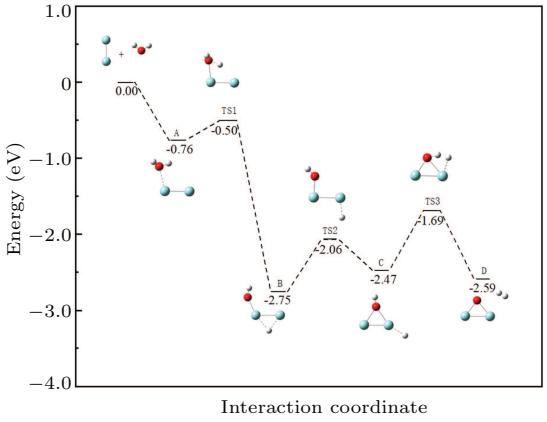


Fig. 4. Reaction paths between Zr_2 and H_2O.

For Zr_3@H_2O, as shown in Fig. 5, the strongest interaction between Zr_3 and H_2O is due to the charge transfer of LPO_4 →LP*Zr_2, which is much stronger than that of BDO_4-H_5/BDO_4-H_6 →LP*Zr_2 . As shown in Fig. 6, the complete reaction process of Zr_3 and single water molecule can be divided into six steps, which are described as follows: first, an OH bond of the molecule is broken, then the dissociated H atom gradually moves away from the O atom, and finally the remaining OH radical is adsorbed between two Zr atoms of the Zr_3 cluster. The activation energy of the reverse reaction of the first transition state is as high as 3.24 eV, so this step is easy to react and not easy to rebound. In the second step, the dissociated H atom is initially located in the plane composed of Zr_3, and gradually moves to the same plane as the plane where Zr_3 lies. Then, the H atom transfers to the lower plane and forms the intermediate product C. In the third, fourth, and fifth stages, the OH radical constantly exchanges adsorption sites with the three Zr atoms. It can be seen that the dissociation of the second H atom is relatively difficult. It is not until the sixth step that the second OH bond begins to break, and the two H atoms approach each other to form hydrogen, releasing 3.45 eV of energy.

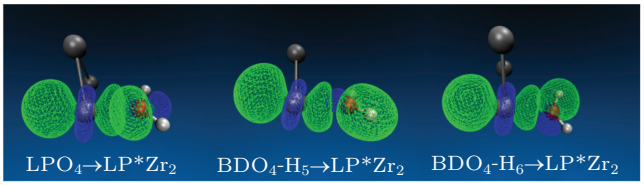


Fig. 5. Main NBO donor–acceptor overlaps between Zr_3 and H_2O.

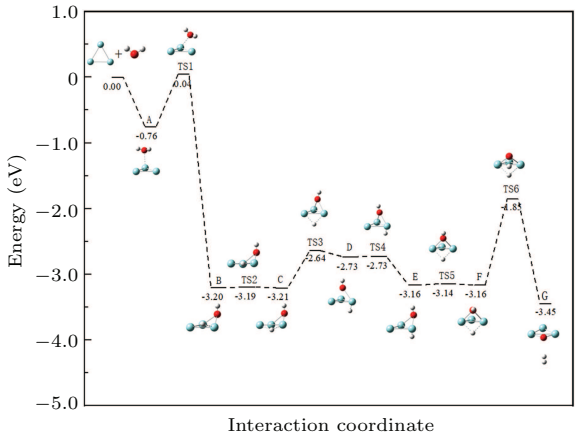


Fig. 6. Reaction paths between Zr_3 and H_2O.

For Zr_4@H_2O, as seen in Fig. 7, the strongest interaction between Zr_4 and H_2O occurs between LP*H_6/LP*H_7 and LP*Zr_2, which is different from that between Zr_2 and H_2O and between Zr_3 and H_2O, the interaction between O atom and Zr_2 in LPO_5 →LP*Zr_2 is relatively not very strong. The complete reaction process of Zr_4 and single water molecule can be divided into six steps as shown in Fig. 8: In the first step, an OH bond is still relatively easy to break, and the dissociated H atom is adsorbed between two Zr atoms. In the second step, the OH radicals' adsorption sites of OH radicals are constantly modified. In the third step, the second H atom begins to dissociate, forming intermediate D. The fourth and fifth steps are accompanied by the continuous adjustment of the adsorption positions of the two H atoms. It is worth noting that the positions of the two H atoms are exchanged in the fifth step. In the sixth step, two hydrogen atoms move closer to each other

and far away from Zr_4O to form hydrogen, releasing 3.64 eV of energy. At the same time, it can be seen intuitively from the potential energy surface that the bond length between hydrogen molecule and Zr_4O is larger than any of Zr_nO ($n = 2$, 3, and 5).

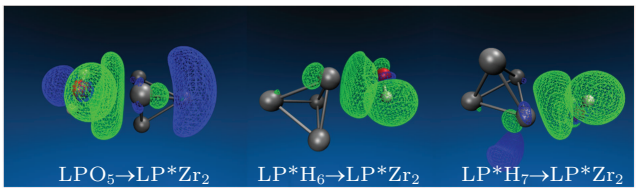


Fig. 7. Main NBO donor–acceptor overlaps between Zr_4 and H_2O.

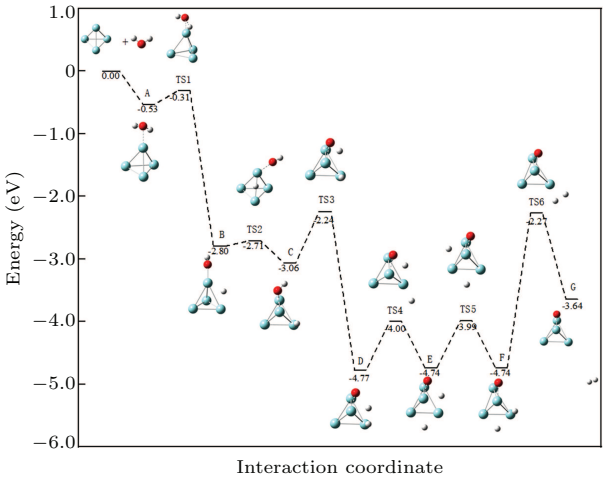


Fig. 8. Reaction paths between Zr_4 and H_2O.

For $Zr_5@H_2O$, as shown in Fig. 9, the strongest interaction between Zr_5 and H_2O occurs between LPO_6 and LP^*Zr_1, but the interactions between LP^*H_7/LP^*H_8 and RY^*Zr_1 electronic transfer are relatively weak. Comparing with Zr_2, Zr_3, and Zr_5, the reaction process of Zr_5 and water is relatively complicated. As shown in Fig. 10, the reaction is divided into eight steps. In the first step, an OH bond is still broken and the dissociated H atom is adsorbed on the Zr_5 cluster. In the second, third, and fourth steps happen mainly the changes of the adsorption sites of H atoms and OH radicals. Therefore, in the second, third, and fourth steps of the reaction, the change of energy is not obvious. The second OH bond does not break until the fifth step. In this step, the energy barrier drops obviously. It should be noted that in the process from TS6 to intermediate product G, the energy barrier is extremely low, only 0.001 eV, which is not shown in Fig. 10. The reaction process of the seventh and eighth steps only involves the change of the position of the H atom, so the energy change is still very small, and finally hydrogen and Zr_5O are formed. The energy of 3.19 eV is released in the whole reaction process.

Table 2 lists the energy barrier for each transition state according to the reaction routes. In the reaction of Zr_n ($n = 2$–5) clusters with single water molecule, there are 3, 6, 6, and 8 transition states, respectively. The energy barriers of rate-determining step are 0.78 eV, 1.31 eV, 2.47 eV, and 1.52 eV, respectively. The Zr_2 cluster reaction with single water molecule, obviously, has the fewest transition states and the lowest rate-determining step energy barrier. Therefore, the interaction of Zr_2 with single water molecule may be thought of as the strongest in the four processes. By carefully comparing the results, it can be said that as the size of the clusters increases, the reaction rate of Zr_n ($n = 2$–5) with single water molecule becomes slower. Among them, 2.59 eV, 3.45 eV, 3.64 eV, and 3.19 eV of energy are released, respectively. The reaction of Zr_4 with single water molecule is the most effective in terms of energy release.

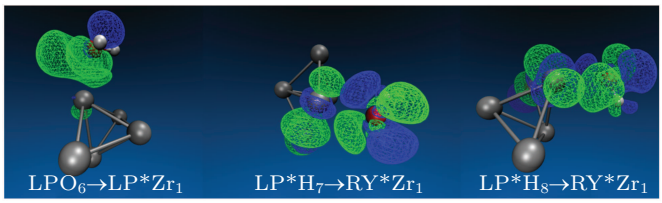


Fig. 9. Main NBO donor–acceptor overlaps between Zr_5 and H_2O.

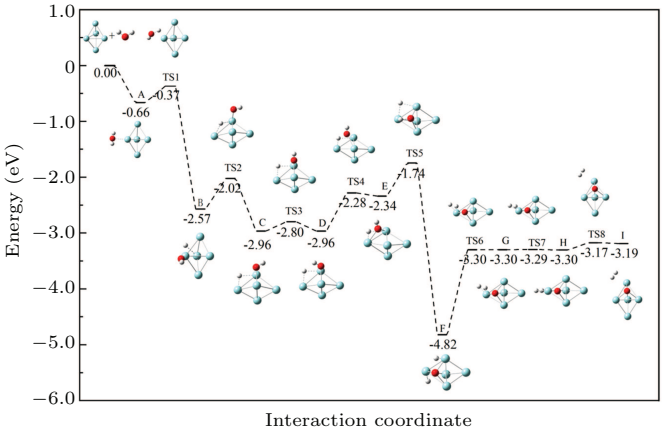


Fig. 10. Reaction paths between $Zr_5$and H_2O.

Table 2. Energy barriers of Zr_n ($n = 2$–5) clusters reacting with single water molecule.

Reaction	Eb_1 (eV)	Eb_2 (eV)	Eb_3 (eV)	Eb_4 (eV)	Eb_5 (eV)	Eb_6 (eV)	Eb_7 (eV)	Eb_8 (eV)
Zr_2+H_2O	0.26	0.69	0.78					
Zr_3+H_2O	0.80	0.01	0.57	0.01	0.02	1.31		
Zr_4+H_2O	0.22	0.09	0.82	0.77	0.75	2.47		
Zr_5+H_2O	0.29	0.55	0.16	0.68	0.60	1.52	0.01	0.13

3.3. Electronic properties of product stable structures

We calculated the natural population analysis (NPA) and density-of-states (DOS) to better understand the product. As shown in Fig. 11, the negative charges are mainly concentrated on the oxygen atoms, whereas the positive charges are mainly accumulated on the atoms adsorbed by the O atoms. This means that the dissociation of H atoms relies heavily on the adsorption of O atoms by the cluster, and the O atoms need to be adsorbed between at least two Zr atoms to be fixed. It can be seen from the figure that only the hydrogen generated by the reaction of Zr_4 with water has no charge, and the H_2 generated by the dissociation of Zr_n ($n = 2$, 3, 5) with water has some positive and negative charges. In addition, considering that the common valence state of the Zr atom is +2 and the highest oxidation state is +4, it can be seen from the figure that the Zr atom in Zr_nO is far from the common valence state or the maximum oxidation state, and there are still many valence electrons that can participate in the reaction. Therefore, we speculate that Zr_nO has the possibility of continuing to extract hydrogen from other water molecules, which deserves further study.

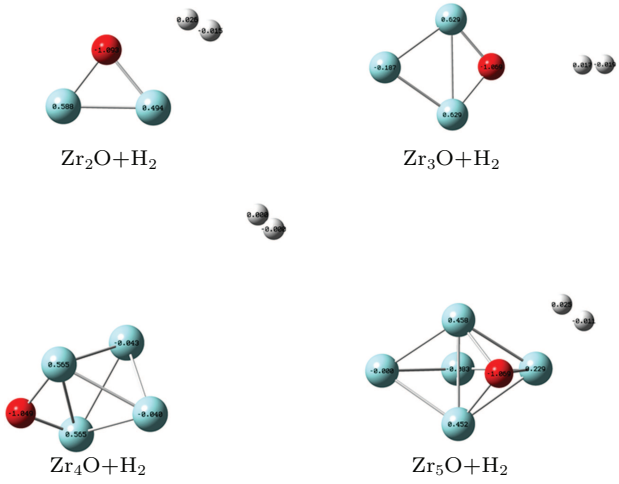


Fig. 11. NPA charges of product.

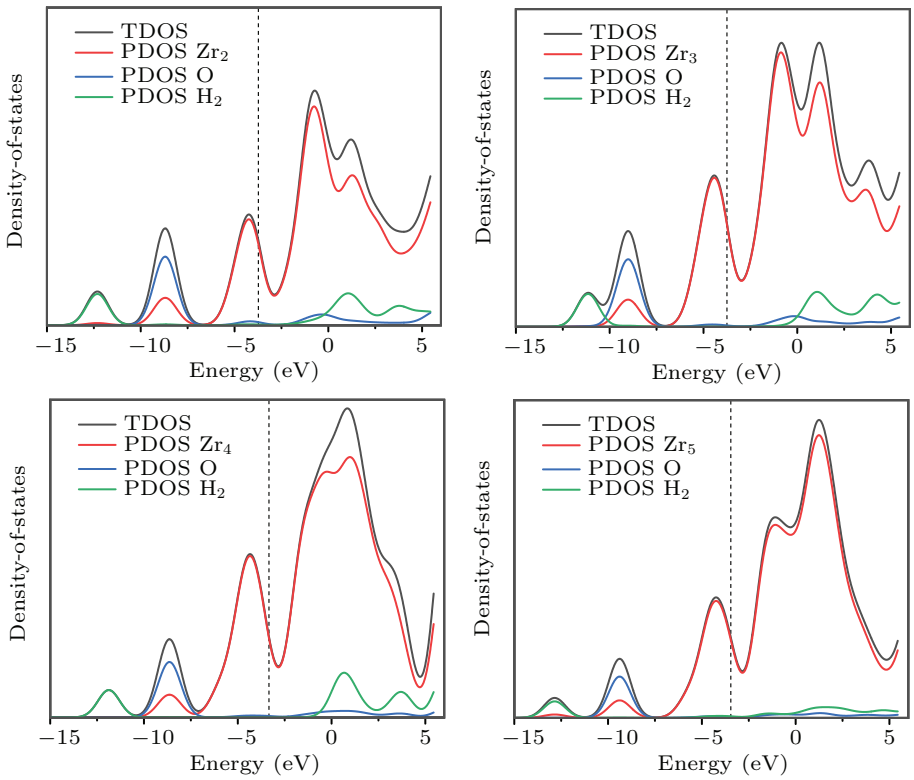


Fig. 12. Curves of density-of-states of products.

The DOS graphs of the product were drawn by Multiwfn 3.7 programs[41] and are shown in Fig. 12, which includes the total DOS of the product (TDOS) and the partial DOS of the constituent product (PDOS). The DOS graphs clearly demonstrate the properties of orbitals in different energy ranges, with extremely similar contributions to TDOS from each PDOS of the four product structures. The first peak is mainly contributed by H_2, the second peak is jointly contributed by the three parts, and the other peaks are mainly contributed by Zr_n ($n = 2$–5). In addition, the Fermi levels of the four product structures all pass through the middle of the energy band, indicating that the electrons are not fully occupied and the products still exhibit the properties of metals. As can be seen, none of the DOSs between the two peaks on both sides of the Fermi level of the four product structures is zero but each DOS peak has a considerable width, which can indicate that the system is composed of covalent bonds. It is further explained that the individual atoms that make up the system do not yet reach the

highest valence. The product may continue to react with other water molecules, which confirms the conclusion drawn from the NPA analysis.

4. Conclusions

In summary, the most stable structures of Zr_n ($n = 2$–5) clusters are predicted by DFT calculations at the level of B3LYP/LANL2DZ (6-311++G (3df, 3pd) of H and O), and the chemical reaction of single water molecule with Zr_n ($n = 2$–5) clusters is theoretically studied by the reaction path search method. The stable structures of Zr_n ($n = 2$–5) clusters after adsorbing water molecules, the adsorption energy of the stable structure and the correlation coefficient between the adsorption energy and the cluster energy gap are calculated. The results show that there is a strong negative linear relationship between the cluster energy gap and the adsorption energy. In addition, the prediction of the reaction path of Zr_n ($n = 2$–5) clusters with single water molecule is also discussed. Our results show that Zr_n ($n = 2$–5) clusters can extract hydrogen completely from water and release 2.59 eV, 3.45 eV, 3.64 eV, and 3.19 eV of energy, respectively. According to the released energy, the Zr_4 cluster is the most efficient in Zr_n ($n = 2$–5) clusters reacting with single water molecule. Our findings provide a more in-depth understanding of the chemical reactions of Zr, which may lead to the subsequent development of efficient Zr-based catalysts.

Acknowledgements

Project supported by the Open Research Fund of Computational Physics Key Laboratory of Sichuan Province, Yibin University, China (Grant No. YBXYJSWL-ZD-2020-005) and the Student's Platform for Innovation and Entrepreneurship Training Program, China (Grant No. S202110616084).

References

[1] Guvelioglu G H, Ma P, He X, Forrey R C and Cheng H 2006 *Phys. Rev. B* **73** 155437
[2] Nie A H, Wu J P, Zhou C G, Yao S J, Forrey, R C and Cheng H 2007 *Int. J. Quantum Chem.* **10** 7219
[3] Yin Q K, Yang C L, Wang M S and Ma X G 2021 *J. Mater. Chem. C* **9** 12231
[4] Zhang C F, Yang C L, Wang M S and Ma X G 2022 *J. Mater. Chem. C* **10** 5474
[5] Wang F, Yang C L, Wang M S and Ma X G 2022 *J. Power Sources* **532** 231352
[6] Sun R, Yang C L, Wang M S and Ma X G 2022 *J. Power Sources* **547** 232008
[7] Zhou R L, Yang Y, Pande S, Qu B Y, Li D D and Zeng X Z 2019 *Phys. Chem. Chem. Phys.* **21** 4006
[8] Lei J L, Shi S P, Guo W, Wan M J, Yan M, Liu Y L and Li X 2021 *Int. J. Hydrog. Energy* **46** 12693
[9] Li K N, Yang C L, Han Y X, Wang M S, Ma X G and Wang L Z 2021 *Energy* **106** 131
[10] Li K N, Yang C L, Wang M S, Ma X G and Wang L Z 2016 *Int. J. Hydrog. Energy* **41** 17858
[11] Sheng X F, Zhao G F and Zhi L L 2008 *J. Phys. Chem. C* **112** 17828
[12] Chen P, He X H, Pang M B, Dong X T, Zhao S and Zhang W 2020 *Appl. Mater. Interfaces* **12** 20429
[13] Duan Z G. Yang H L, Satoh Y, Murakami K, Kano S, Zhao Z S, Shen J J and Abe H 2017 *Nucl. Eng. Des.* **316** 131
[14] Kim H G, Yang J H, Kim W J and Koo Y H 2016 *Nucl. Eng. Technol.* **48** 1
[15] Ribis J, Wu A and Brachet J C 2018 *J. Mater. Sci.* **53** 9879
[16] Zinkle S J and Was G S 2013 *Acta Mater.* **61** 735
[17] Wei Z, Zhai D, Shao X H, Lu Y and Zhang P 2015 *Chin. Phys. B* **24** 043102
[18] Srikanth M, Annamalai A R, Muthuchamy A and Jen C P 2021 *Crystals* **11** 612
[19] Yang X Y, Lu Y, Zheng F W and Zhang P 2015 *Chin. Phys. B* **24** 116301
[20] Fahrenholtz W G and Hilmas G E 2017 *Scr. Mater.* **129** 94
[21] Montesinos-Castellanos A and Zepeda T A 2008 *Microporous Mesoporous Mat.* **113** 146
[22] Skoda D, Styskalik A and Moravec, Z 2015 *J. Mater. Sci.* **50** 3371
[23] Fernández-Morales J M, Lozano L A, Castillejos-López E, Rodríguez-Ramos I, Guerrero-Ruiz A and Zamaro J M 2019 *Microporous Mesoporous Mat.* **290** 109686
[24] Narayanan S, Krishnan M S and Vishwanathan V 1995 *J. Mater. Sci.* **30** 6355
[25] Khann M A, Wang N, Zhang L H, Guo X Y and Huang S P 2020 *Comput. Theor. Chem.* **188** 112940
[26] Syzgantseva O, Calatayud M and Minot C 2011 *Chem. Phys. Lett.* **503** 12
[27] Wang F and Gong H R 2012 *Int. J. Hydrog. Energy* **37** 9688
[28] Wang C C, Zhao R N and Han J G 2006 *J. Chem. Phys.* **124** 194301
[29] Wang X Q, Jiang Z Y, Li J Q, He Q L and Chu S Y 2011 *Int. J. Quantum Chem.* **111** 182
[30] AD B 1993 *J. Chem. Phys.* **98** 5648
[31] A D B 1998 *Phys. Rev. A* **38** 3098
[32] Lee C, Yang W and Parr R G 1988 *Phys. Rev. B* **37** 785
[33] Bandyopadhyay D 2008 *J. Appl. Phys.* **104** 084308
[34] Bandyopadhyay D and Kumar M 2008 *Chem. Phys.* **353** 170
[35] He C, Chen L and Sheng Y 2019 *Eur. Phys. J. D* **73** 90
[36] Jin R and Chen X H 2010 *Acta Phys. Sin.* **59** 6955 (in Chinese)
[37] Kagdada H L, Dabhi S D, Mankad V, Shinde S M and Jha P K 2020 *Mater. Chem. Phys.* **239** 122264
[38] Krishnan R, Seeger B J and Pople J A 1980 *J. Chem. Phys.* **72** 650
[39] Frisch M J, Trucks G W, Schlegel H B, *et al.* 2016 *Gaussian* 16 *Revision A*.03
[40] Glendening E D, Reed A E, Carpenter J E and Weinhold F 2009 *NBO Version* 3.1
[41] Lu T and Chen F W 2012 *J. Comput. Chem.* **33** 580
[42] Humphrey W, Dalke A and Schulten K 1996 *J. Mol. Graph.* **14** 33